

OBSERVATIONS OF MOLECULAR AND ATOMIC GAS IN
PHOTODISSOCIATION REGIONS

D.T. Jaffe and J.E. Howe

University of Texas at Austin

RESUMEN. El gas denso en las fronteras ionizadas/neutras de las nubes moleculares que están iluminadas por fotones en el lejano ultravioleta juega un papel importante en la apariencia del medio interestelar neutro. También es un laboratorio para el estudio de la fotoquímica ultravioleta y de un número de fenómenos de calentamiento y enfriamiento que no se observan en otros sitios. Las líneas de estructura fina de especies neutras y de bajo potencial de ionización dominan el enfriamiento en la parte externa de las regiones de fotodisociación. Las observaciones de estas líneas muestran que las regiones son densas y altamente inhomogéneas. Las observaciones de H_2 y CO muestran que el calentamiento por fotones *UV* juega un papel significativo en la excitación de líneas moleculares cerca de la frontera H II/región neutra. El CO tibio es más abundante en estas regiones que lo predicho por los modelos teóricos estándar – ya sea como resultado de densidades muy altas cerca de las regiones de la frontera o como resultado de un mecanismo desconocido de calentamiento en el interior de la nube. Las nebulosas ópticas de reflexión son laboratorios ideales para el estudio de los fenómenos característicos de las regiones de fotodisociación.

ABSTRACT. Dense gas at the ionized/neutral boundaries of molecular clouds illuminated by far-*UV* photons plays an important role in the appearance of the neutral interstellar medium. It also is a laboratory for the study of *UV*-photochemistry and of a number of heating and cooling phenomena not seen elsewhere. Fine structure lines of neutral and low ionization potential species dominate the cooling in the outer part of the photodissociation regions. Observations of these lines show that the regions are dense and highly clumped. Observations of H_2 and CO show that heating by *UV* photons plays a significant role in the excitation of molecular lines near the H II/neutral boundary. Warm CO is more abundant in these regions than predicted by the standard theoretical models – either as a result of very high densities near the boundary regions or as the result of an unknown heating mechanism farther into the cloud. Optical reflection nebulae provide an ideal laboratory for the study of photodissociation region phenomena.

Key words: INTERSTELLAR-CLOUDS — INTERSTELLAR- MOLECULES

I. INTRODUCTION

Photodissociation regions (PDRs) are the boundary layers of molecular clouds where ultraviolet and far-UV photons at $\lambda > 91$ nm dominate the energetics, ionization balance, and chemical processes in the gas. These neutral or partially ionized regions exist at the outer edges of clouds exposed to a wide range of ultraviolet radiation fields. The UV radiation affects the boundaries of isolated dark clouds which receive only the ultraviolet flux from the general interstellar radiation field ($G_0 = 1.6 \times 10^{-3}$ erg cm $^{-2}$ s $^{-1}$, 91 nm $< \lambda < 300$ nm; Habing 1968) and has a significant influence in molecular clouds bordering compact H II regions, which may intercept a flux as large as 10^5 - 10^6 G_0 . To the specialist in ionized nebulae, the study of PDRs affords an opportunity to investigate the physics and structure of the region immediately outside the boundary of H II regions and can also serve as a framework for studies of very low ionization nebulae in dense gas surrounding B type stars. To the molecular cloud specialist, the PDRs offer new information about the physics, chemistry, and structure of molecular clouds. In some situations, particularly in giant molecular clouds where OB star formation is already taking place and in the inner regions of starburst galaxies where the mean interstellar radiation field can approach 10^3 G_0 , enough of the interstellar material may be in PDRs to have an effect on the global appearance of the region and on global characteristics such as the star formation rate.

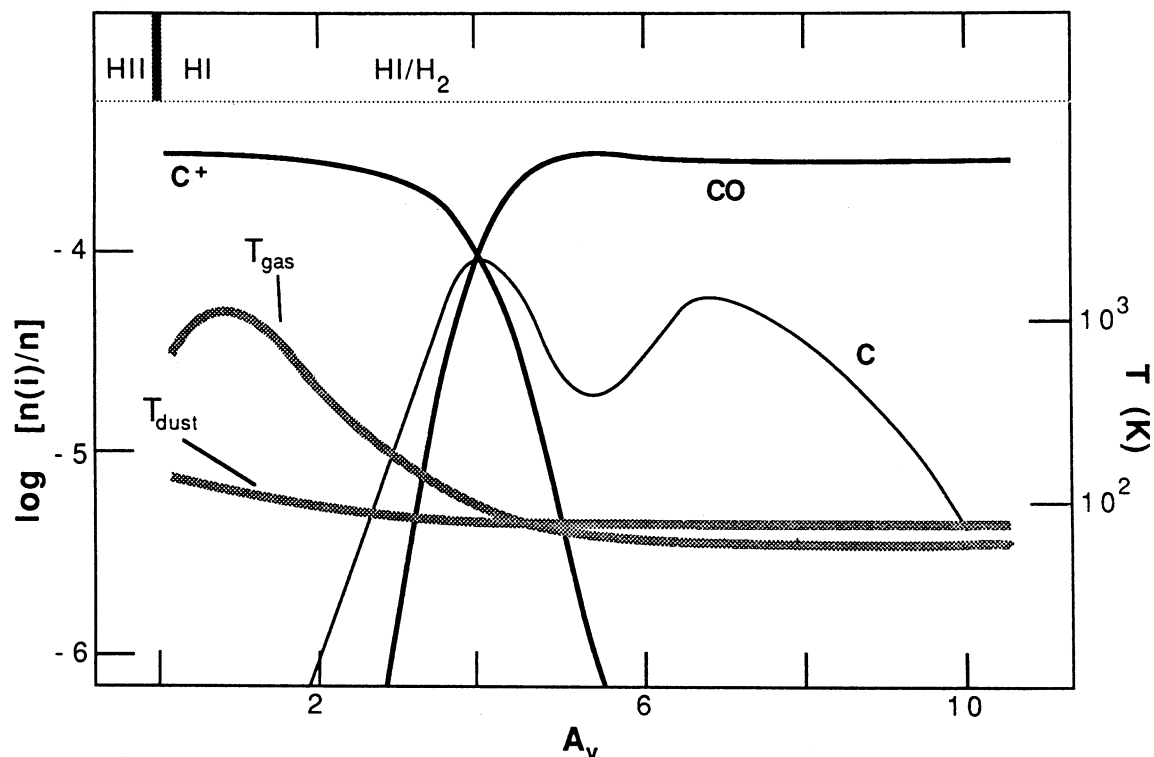


Fig. 1 : Schematic model of a photodissociation region. The abundance of carbon species i , $n(i)/n$ (left scale), and the gas and dust temperature (right scale) are plotted as a function of visual extinction A_v into the predominantly neutral gas (adapted from Tielens and Hollenbach 1985). The plotted quantities are based on the Tielens and Hollenbach (1985) standard model. The top of the diagram outlines the approximate state of hydrogen versus depth into the cloud.

Most observational studies of PDRs have been at infrared and submillimeter wavelengths both because the major cooling lines are in this range and as a result of the significant optical and UV extinction present even in nearby PDRs. Section II contains a summary of the theoretical models of PDRs. Section III discusses the nature of the atomic component of the PDR. Section IV discusses the warm molecular gas in these regions and Section V presents recent results on studies of PDRs in optical reflection nebulae. Section VI summarizes the major points.

II. THEORETICAL PICTURE OF PDR's

In regions near strong ultraviolet sources, the H II region/neutral cloud boundary forms the outer edge of the photodissociation region. The inner (less well-defined) transition to a normal molecular cloud occurs where the extinction due to the dust (which controls the flow of UV photons into the cloud) has reached an $A_v = 6-10$ and the influence of UV photons on the chemistry and energetics of the region is no longer significant. Models of PDRs must take into account heating and cooling mechanisms, ionization balance, and the photochemistry of abundant elements like hydrogen, carbon and oxygen. Early PDR models included many of these features (e.g., Pankonin and Walmsley 1976) and successfully predicted the high gas temperatures in the regions. Tielens and Hollenbach (1985) present a detailed one-dimensional physical and chemical model of photodissociation regions. Figure 1 illustrates their model schematically. In the "standard" model, constructed for a dense ionization front region like the Orion bar ($G = 10^5 G_0$, $n = 2 \times 10^5 \text{ cm}^{-3}$), carbon is primarily in the form of C^+ at $A_v < 4$ and is tied up in CO at $A_v > 4$. Neutral atomic carbon is nowhere the dominant form, but exists in substantial abundance from $A_v = 2$ to $A_v = 8$. In the outer part of the PDR ($A_v < 2$), the ultraviolet photons heat the gas significantly above the dust temperature, to temperatures as high as 10^3 K . The most important heat source for the gas is electrons ejected photoelectrically from grain surfaces (Spitzer 1948; Watson 1972). The photoelectrons typically deposit a few tenths of a percent of the incident UV energy into the gas (Tielens and Hollenbach 1985). Another, less significant heat source at $A_v < 2$ is H_2 vibrational heating. Ultraviolet fluorescence leaves molecular hydrogen in excited vibrational states of the ground electronic state. At high densities and temperatures ($n_{\text{H}_2} \geq 10^6 \text{ cm}^{-3}$ for $T = 400 \text{ K}$), a significant fraction of the excited H_2 molecules will be de-excited collisionally, transferring several eV to the gas with each collision (Hollenbach 1988; Sternberg 1986; Tielens and Hollenbach 1985). Farther into

the cloud, dust grains dominate the heating through collisions and indirectly through far-IR excitation of O I, and the gas temperature is less than the dust temperature.

Infrared fine structure lines arising from the ground states of O I and C II dominate the cooling in the outer part of the PDR (see, e.g., Dalgarno and McCray 1972). The PDR models predict an approximately logarithmic dependence of emergent intensity of the $158\ \mu\text{m}\ 2^2\text{P}_{3/2} \rightarrow 2^2\text{P}_{1/2}$ line of [C II] on the strength of the incident UV field. Since dust absorbs most of the UV energy, a linear increase in the depth of the C⁺ region requires an exponential increase in incident UV flux. The C⁺ line-strength therefore depends only weakly on G above $10^3\ G_0$. The PDR chemistry models (Tielens and Hollenbach 1985) predict that at densities $\lesssim 10^5\ \text{cm}^{-3}$, the abundance of CO will be very low in the region at $A_V < 2$ where the gas temperature is significantly higher than the dust temperature. Newer data on the CO photodissociation processes imply an even lower abundance of CO at $A_V < 2$ for PDR models with $G = 10^4\ G_0$ and $n = 10^4\ \text{cm}^{-3}$ (van Dishoeck and Black 1988). Farther into the cloud ($A_V > 5$), rotational transitions of CO and the ground state fine structure lines of neutral carbon are the primary gas coolants. In the Tielens and Hollenbach models, the emergent flux in the [C I] lines is only weakly dependent on G for $G > 10\ G_0$ for reasons similar to the cause of the weak G dependence of [C II] intensity at higher values of G/G₀.

III. ATOMIC GAS IN PHOTODISSOCIATION REGIONS

a) Structure

The $158\ \mu\text{m}$ line of C⁺ is the most unambiguous tracer of dense photodissociation regions both because this line is a major coolant in such regions and because it is not a strong cooling line in shocked regions. The transition has a critical density for neutral collisions of a few $10^3\ \text{cm}^{-3}$ and requires UV fluxes in excess of $\sim 10^2\ G_0$ to be detectable with current sensitivity. The [C II] line is widely distributed in our own Galaxy (Stacey *et al.* 1985; Russell *et al.* 1981) and in external galaxies (Crawford *et al.* 1985). An analysis of the possible origin of this emission

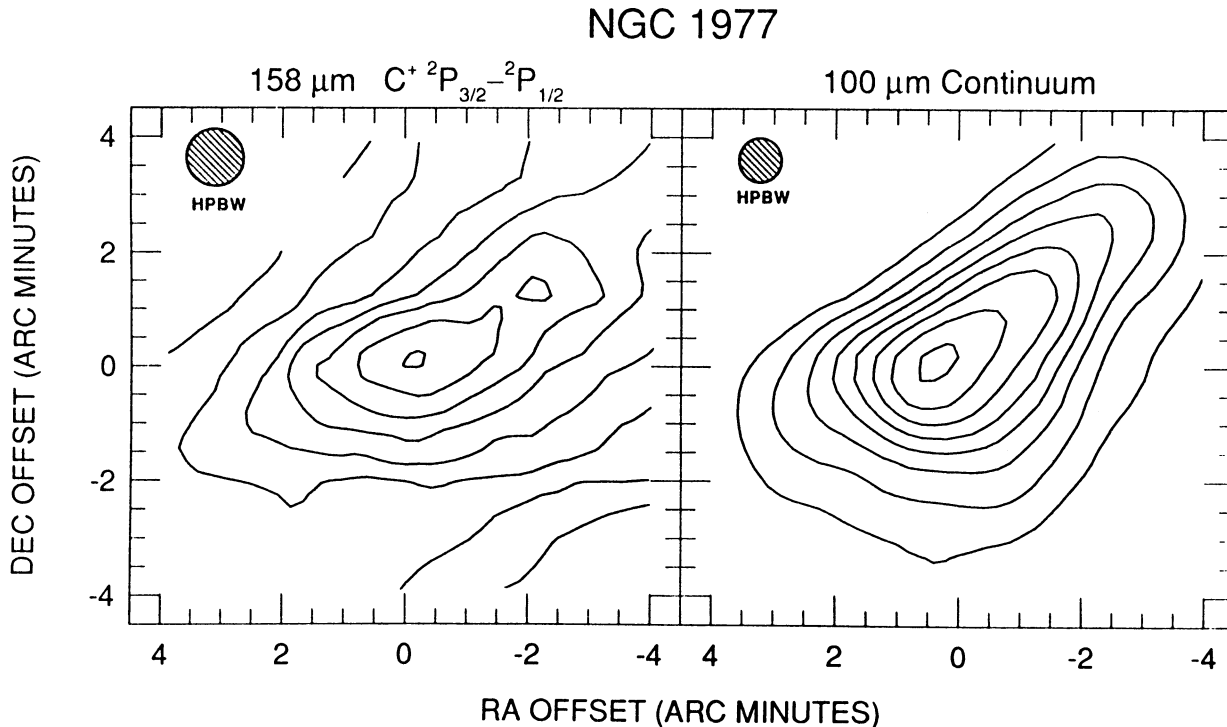


Fig. 2: Maps of the integrated $158\ \mu\text{m}$ [C II] emission (Howe *et al.* 1989) and $100\ \mu\text{m}$ continuum emission (Makinen *et al.* 1985) from the H II region/molecular cloud boundary in NGC 1977. (0,0) = $5^{\text{h}}32^{\text{m}}44^{\text{s}}, -04^{\circ}57'00''$. The exciting star 42 Ori is at ($2^{\circ}.8\text{E}, 4^{\circ}.8\text{N}$). [C II] contours are 20 to 90 percent of the peak flux of $1.5 \times 10^{-17}\ \text{W cm}^{-2}$. The $100\ \mu\text{m}$ continuum contours are 20 to 90 percent of the peak surface brightness of $330\ \text{Jy beam}^{-1}$. Contour intervals are 10 percent for both maps. In the [C II] map, continuum emission contributes < 15 percent of the total flux.

demonstrates that PDRs dominate over other sources of C^+ line flux such as H II regions and H I clouds. Locally near OB star clusters, C II extends over regions of 3-10 pc (Stutzki *et al.* 1988; Howe *et al.* 1989). The observed C^+ column densities are $\sim 10^{18} \text{ cm}^{-2}$, consistent with a single layer extending into the clouds to an A_V of a few. Mapping results show that the region of largest C II brightness coincides with the region where the most energy is deposited in the dust and re-radiated in the far-IR. Figure 2 shows a comparison of a [C II] 158 μm line map and a 100 μm continuum map of the ionization front in NGC 1777 (Howe *et al.* 1989; Makinen *et al.* 1985). The scale length of the [C II] emission dropoff into the cloud here is ~ 10 times larger than predicted by the 1-d models. Recent observations of [C II] in M17 (Stutzki *et al.* 1988) show that the emission peaks between the ionized region and the adjacent dense molecular cloud and decreases into the cloud over a scale-length of ~ 2 pc. Based on both the cloud density determined from molecular line observations ($\geq 4 \times 10^4 \text{ cm}^{-3}$) and the far-IR optical depth, this scale-length corresponds to $A_V \sim 100$.

A high degree of clumping in the PDR can explain the apparent contradiction between the 1-d models and the observed scale-length of the C^+ emission. If carbon ionizing photons penetrate into a low density medium between dense molecular clumps in the interface, the mean UV flux at a point in the interface is given by

$$F = \frac{L}{4\pi R^2} \exp \left[- \left(\frac{\phi_v}{D_C} \right) (R - R_0) \right] \quad (1)$$

(Stutzki *et al.* 1988) where ϕ_v is the volume filling factor and D_C the diameter of the clumps, R the distance from the OB stars with luminosity L , and R_0 the radius of the H II region. Comparisons of beam averaged column densities and densities derived from excitation calculations (Stutzki *et al.* 1988) as well as direct observations of clumps in $C^{18}O$ (Stutzki and Guesten 1989) give a volume filling factor of 0.1 to 0.4. The resulting value of D_C/ϕ_v , the scale-length for the penetration of UV flux into the cloud is therefore 1-2 pc. Figure 3 shows a comparison of the observed [C II] distribution in M17 to the emission predicted from a UV field given by equation 1 (model II in figure 3) or under the assumption that the scattering at the clump surfaces merely redistributes the incident radiation (model I) coupled with the standard Tielens and Hollenbach 1-dimensional PDR [C II] excitation models (Stutzki *et al.* 1988). Clearly, a clumpy cloud with some degree of UV scattering by dust can provide a good explanation of the [C II] results in the context of the PDR picture.

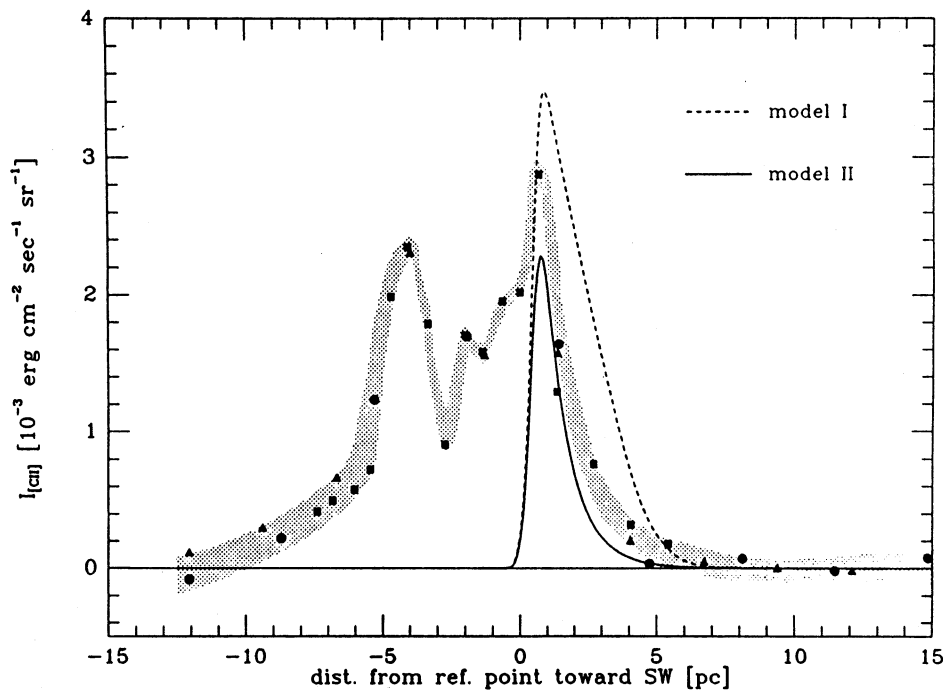


Fig. 3 : The observed [C II] intensity distribution in M17 (filled circles, squares, and triangles) as a function of distance from the OB star cluster (from Stutzki *et al.* 1988) compared to theoretical models for a clumpy medium penetrated by UV radiation (models described in text).

The disagreement between theory and observation is also significant for the [C I] lines. Observations of C^0 show that it is more abundant than predicted by the one dimensional PDR models (Phillips and Huggins, 1981) and extends well away from the H II/H₂ boundary into the molecular cloud (Keene *et al.* 1985). The high abundance and large spatial extent of the C^0 were initially explained by non-equilibrium chemical models of molecular clouds in which the steady-state situation, where the carbon is completely tied up in CO, has not been reached (e.g. Langer 1976; Iglesias 1977; Gerola and Glassgold 1978; Graedel, Langer, and Frerking 1982; see also Keene *et al.* 1985; Frerking *et al.* 1989). High spatial resolution observations of the $370 \mu\text{m } ^3P_2 \rightarrow ^3P_1$ transition of [C I] in the M17 interface (Genzel *et al.* 1988), however, support the clumpy PDR model for the [C I] as well as the [C II] emission. The [C I] mapping results show a strong spatial correlation between the $C^{18}O 2 \rightarrow 1$ line and the upper [C I] ground state transition. For all points observed, there is a linear correlation of [C I] line strength with $C^{18}O 2 \rightarrow 1$ strength at low values of $I(C^{18}O)$, the intensity of the $C^{18}O$ emission, which weakens somewhat at $I(C^{18}O) > 50 \text{ K km s}^{-1}$. The data shown imply $N(C I) \sim 0.2 N(CO)$ (Genzel *et al.* 1988). The spatial correlation is expected if the [C I] arises in the outer layers of the same clumps as the $C^{18}O$ emission. The linear relation in intensities reflects the ability of the beam averaged $C^{18}O$ column density to count the number of clumps (and therefore the number of small PDRs) in each beam. For exceptionally large or dense clumps, the $C^{18}O/[C I]$ ratio will be smaller than typical, leading to the observed saturation effect.

While the scale-length for [C I] emission is longer than for [C II] due to the very weak dependence of $I([C I])$ on the local value of G , the clumpy cloud model cannot explain the full spatial extent of the [C I] in clouds like Orion and M17 if only the central OB cluster excites the gas. The lower-level extended emission must depend on an incident UV flux higher than the mean interstellar radiation field value incident on the clouds or arising from young stars within them. Observed embedded sources like the B star clusters in the M17 cloud (Jaffe and Fazio 1982), or fully emerged OB associations nearby, can supply the necessary UV.

b) Excitation

O I and C II are the dominant forms of carbon and oxygen in the primarily atomic part of the PDR. We can use the three ground-state fine-structure lines of O^0 and C^+ to derive the physical conditions in the outer layers of the PDRs. Table I lists the relevant parameters for these lines as well as those of C I. Collisions with H or H₂ populate the fine structure levels in the ground states of these atoms which are then de-populated either collisionally or radiatively. The critical densities (n_{crit} is the density at which the number of downward radiative and collisional transitions are equal) and energy above ground differ strongly for the three lines (see Table 1). It is possible, therefore, to use ratios between the [OI] and [C II] lines to derive the temperature and density in the neutral region (Fig. 4). Estimates of the excitation in the atomic gas have been made for Orion ($n_{\text{H}}T \sim 3 \times 10^7 \text{ cm}^{-3} \text{ K}$; Stacey *et al.* 1983), M17 ($n_{\text{H}}T \sim 1 \times 10^7 \text{ cm}^{-3} \text{ K}$; Stutzki *et al.* 1988), the ring around the Galactic Center ($n_{\text{H}}T \sim 3.5 \times 10^7 \text{ cm}^{-3} \text{ K}$; Genzel *et al.* 1985) and for M82 ($n_{\text{H}}T \sim 3 \times 10^6 \text{ cm}^{-3} \text{ K}$; Lugten *et al.* 1988). In some cases, radiative transfer effects can complicate the derivation of temperature and density. In the C^0 region, where only two lines are available and where these lines are easily thermalized, fine structure lines do not provide much excitation information.

Table 1: Fine Structure Transitions

Species	Transition	$\lambda(\mu\text{m})$	$E_u(\text{K})$	$A_{ul}(\text{s}^{-1})$	$n_{\text{crit}}(\text{cm}^{-3})$
C^0	$^3P_1 \rightarrow ^3P_0$	609.1	24	7.93×10^{-8}	5×10^2
	$^3P_2 \rightarrow ^3P_1$	370.4	63	2.68×10^{-7}	3×10^3
C^+	$^2P_{3/2} \rightarrow ^2P_{1/2}$	157.7	92	2.4×10^{-6}	4×10^3
O^0	$^3P_1 \rightarrow ^3P_2$	63.2	228	8.95×10^{-5}	5×10^5
	$^3P_0 \rightarrow ^3P_1$	145.5	326	1.70×10^{-5}	1×10^5

IV. WARM MOLECULAR GAS

The distribution and excitation of the dominant molecular species, H₂, and the abundant tracer molecule, CO, are important to our overall understanding of PDRs. Molecular hydrogen is difficult to photodissociate both because of its high dissociation energy and as a result of the effective self-shielding made possible by its high abundance. Historically, most observations of H₂ emission from dense interstellar gas have been of near infrared vibrational

transitions in shock excited regions. H_2 vibrational transitions also arise in PDR's as a result of UV fluorescence. Only about 10 percent of UV excitations result in dissociation. The balance are followed by a downward

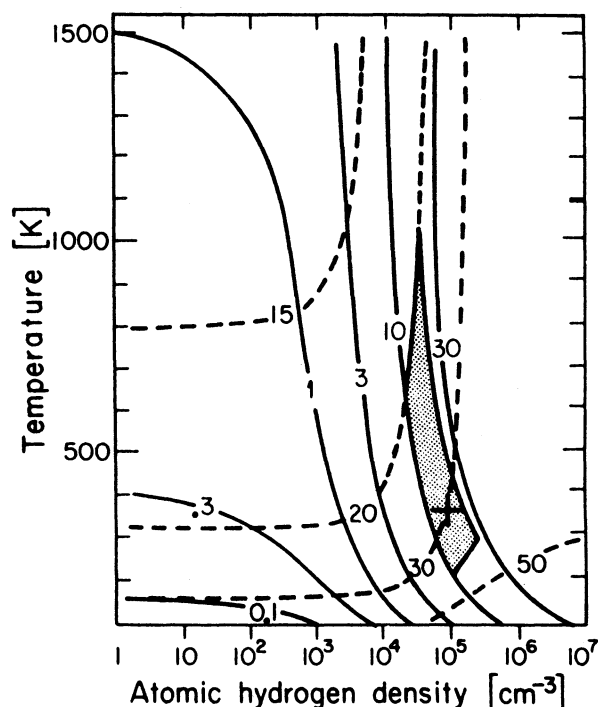


Fig. 4 : Plot of the ratios of constant [O I] 63 μm /[C II] 158 μm line flux (solid lines) and constant [O I] 63 μm /[O I] 146 μm line flux (dashed lines) in the temperature-density plane (from Genzel *et al.* 1985). The cross and shaded region give the line flux ratio value and 1σ error box for one position in the galactic center. An O^+/C^+ abundance ratio of 2.2 and optically thin emission were assumed for this plot.

The lines are narrow ($\Delta v_{7-6} \sim 5 \text{ km s}^{-1}$ in M17, Harris *et al.* 1987; $\leq 1.5 \text{ km s}^{-1}$ in NGC 2023, Jaffe *et al.* 1989b), making heating by shocks extremely unlikely. In regions where several high excitation lines have been measured, we can derive the temperature, density and column density in the emitting gas by comparing the observed variation of intensity with rotational quantum number J to excitation models. Since some transitions may be optically thick, the excitation calculations must include radiative trapping through the escape probability formalism. In general, the ratio of far-IR to submillimeter CO line strengths is very sensitive to the gas pressure $n_{H_2}T$. For the M17 interface, the models imply n_{H_2} a few 10^4 cm^{-3} and $T \sim 250 \text{ K}$ (Harris *et al.* 1987). The narrow CO 17 \rightarrow 16 line in the Orion bar implies similarly high temperatures for that region (Boreiko *et al.* 1988).

The high abundance of warm quiescent CO in interface regions is not in agreement with PDR models with gas densities less than $\sim 10^6 \text{ cm}^{-3}$. The minimum column densities for the warm CO (assuming $\tau \ll 1$) are $\sim 10^{18} \text{ cm}^{-2}$, which would require $N_{H_2} \sim 10^{22} \text{ cm}^{-2}$ of molecular material in the part of the PDR with $T_{\text{gas}} \gg T_{\text{dust}}$. Since the high gas temperatures only extend into the cloud to $A_V \sim 3$ (Tielens and Hollenbach 1985), the high abundance of warm CO requires CO to exist almost to the H II region or cloud boundary. More recent PDR models at higher densities ($n_{H_2} = 10^6\text{--}10^7 \text{ cm}^{-3}$) do predict far-IR and submillimeter CO intensities in agreement with observations (Hollenbach 1988; Burton, Hollenbach, and Tielens 1988). At the higher densities, self-shielding permits CO to exist closer to the cloud boundary. With a more complete treatment of the H_2 fluorescence, the UV- H_2 heating begins to aid greatly in warming the gas.

What are the physical and observational consequences of the high density models for the warm CO in PDRs? The models predict a substantial pressure, of order $10^{8-9} \text{ cm}^{-3} \text{ K}$, in the warm molecular regions (considerably higher

electronic transition leading to a radiative cascade through the vibrational states of the ground electronic state with a spectrum distinctly different from the spectrum of shock excited H_2 . The fluorescent spectrum is characterized by the high strength of transitions arising in states with $v > 1$ (Black and van Dishoeck 1987). UV fluorescent H_2 spectra have been observed in interface regions of reflection nebulae (Sellgren 1986; Gatley *et al.* 1987), and in the neutral shells of planetary nebulae (Dinerstein *et al.* 1988). As mentioned in section II, at high densities, the UV fluorescence becomes a heating mechanism through collisional de-excitation.

Observations of submillimeter and far-infrared rotational transitions of CO have revealed the presence of a new molecular gas component in interstellar clouds. Toward many clouds associated with compact H II regions, the CO $J = 7 \rightarrow 6$ transition (which originates 155 K above ground from a state with critical density $n_{\text{crit}}(J=7 \rightarrow 6) = 6 \times 10^5 \text{ cm}^{-3}$) has a brightness temperature 2-3 times higher than the $J = 1 \rightarrow 0$ line (which originates 5 K above ground with $n_{\text{crit}}(J=1 \rightarrow 0) = 3 \times 10^3 \text{ cm}^{-3}$). Both the CO 7 \rightarrow 6 brightness temperature and the 7 \rightarrow 6/1 \rightarrow 0 intensity ratio indicate a kinetic temperature for the gas significantly above the temperature of the dust radiating at far-IR wavelengths. It is this 30-50 K dust which heats the molecular material in the bulk of the cloud.

The location of the warm CO and the need for an efficient mechanism to heat the gas significantly above the dust temperature both point to a possible association between the new, warm molecular regions and PDR's. The warm gas is morphologically associated with the H II/ H_2 interfaces (Stutzki *et al.* 1988; Jaffe *et al.* 1989a; Schmid-Burgk *et al.* 1989).

than the pressure derived from fine-structure line observations of the same regions). The extent of UV penetration in M17 as traced by the C II emission requires a density contrast of $\geq 10^3$ in the clump/interclump gas to explain the low extinction between the clumps. If the pressure is this high, the dense clumps must be gravitationally bound to prevent expansion which would dissipate them on time scales of 10^4 – 10^5 years (Hollenbach 1988), or it would require an interclump gas temperature $\geq 10^5$ K to pressure-bound the clumps. From an observational perspective, the high densities should also be found in the cooler molecular gas in the PDR. In M17, the area filling factor of the warm CO is $\phi_A \sim 0.2$ – 0.5 (Stutzki *et al.* 1988). The cooler neutral interface material, which must be comparable in density, should have ϕ_A of the same order as the warm CO (CS 6 \rightarrow 5 observations of M17 give $n \sim 10^6$ cm $^{-3}$ and $\phi_V \sim 0.03$ for $T = 50$ K, roughly consistent with such a picture; Snell *et al.* 1984). Rotational transitions of high dipole moment molecules should have appropriately high line strengths in these interfaces. If the high density PDR model is incorrect, there must be an important unknown heating mechanism active at $A_V > 2$ or a CO-shielding mechanism to produce the warm CO.

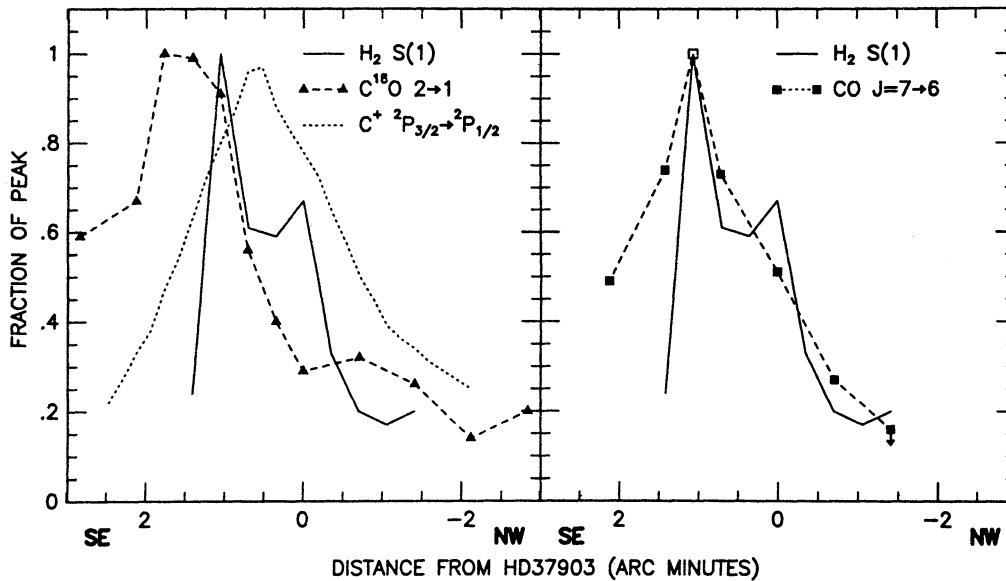


Fig. 5: A one dimensional cut through the reflection nebula NGC 2023. The cut runs from southeast to northwest through the B 1.5 star HD 37903 ($\alpha = 05^h39^m07^s.3$, $\delta = -02^\circ16'58''$ (1950)). All observations are normalized to the peak value. H $_2$ [$v = 1 \rightarrow 0$, S(1)] (2.12 μ m; Gatley *et al.* 1987): Peak line flux = 5×10^{-20} W cm $^{-2}$ in a 19.6 arcsec beam. C 18 O J = 2-1 (1.3 mm): Peak integrated line brightness = 11. K km s $^{-1}$ ($\theta_{\text{BEAM}} = 30$ arcsec). [C II] $^2P_{3/2} \rightarrow ^2P_{1/2}$ (158 μ m): Peak line flux = 8×10^{-18} W cm $^{-2}$ ($\Omega_{\text{BEAM}} = 8.6 \times 10^{-8}$ sr). CO J = 7 \rightarrow 6 (372 μ m): Peak T $_{\text{MB}}$ = 75 K ($\theta_{\text{BEAM}} = 32$ arcsec).

V. REFLECTION NEBULAE AS PDR LABORATORIES

Optical reflection nebulae around B stars are ideal sources for studies of moderately excited PDRs. While ionization fronts often have $G = 10^4$ – 10^5 G_0 , reflection nebulae are more typically in the range $G = 10^2$ – 10^3 G_0 . Since they are close-by, far-IR studies can be carried out with good linear resolution. Chokshi *et al.* (1988) have recently mapped NGC 7023 in the 63 μ m [O I] line and the 158 μ m [C II] line. The line strengths are in good agreement with the models of Tielens and Hollenbach (1985) for appropriate values of G and the maps show that the excitation drops at greater distances from the exciting star.

Jaffe *et al.* (1989b) have studied the reflection nebula NGC 2023 in [C II], CO 7 \rightarrow 6, CO 2 \rightarrow 1 and C 18 O 2 \rightarrow 1 and have compared these results to maps of the $v = 1 \rightarrow 0$ S(1) line of H $_2$ (Gatley *et al.* 1987). The morphology of the region agrees well with the PDR picture, particularly southeast of the B 1.5 V exciting star where the UV radiation illuminates a dense shell of atomic and molecular material. Figure 5 shows cross-cuts running from southeast to northwest through the exciting star. The C $^+$ zone lies close to the star, peaking just to the southeast. An arc of fluorescent H $_2$ emission lies just beyond the [C II] peak followed by a strong peak in the C 18 O 2 \rightarrow 1 emission. The CO 7 \rightarrow 6 peak coincides with the peak in infrared H $_2$ emission. The CO in the interface is considerably hotter ($T_k \geq 90$ K) than the temperature of the far-IR continuum emitting dust grains. The high kinetic temperature implies that whatever mechanism heats the warm molecular gas is still effective at $G \sim 10^3$ G_0 . The extremely narrow (e.g. Fig. 6) CO lines in this region (≤ 0.9 km s $^{-1}$ at one position) effectively eliminate the possibility of shock heating of the gas.

VI. SUMMARY

Photodissociation regions are strong emitters of far-IR atomic fine-structure lines and of submillimeter CO lines. The UV radiation, which dominates the heating in these regions, also gives rise to fluorescent H_2 emission. Recent physical and chemical models of PDRs have successfully predicted most of the observed properties of PDRs. With the possible exception of hot CO, there is good agreement between theory and observation when a clumpy nature to the molecular interface region is included in the picture. The high-temperature, high-density clump regions dominate the emergent far-IR line flux in our galaxy and in other galaxies. The clumpy nature of the molecular gas increases the amount of material that is efficiently heated by UV radiation and the extent of the regions containing ions of easily ionized atoms. In addition to their utility as interstellar laboratories for studies of interesting physical phenomena, PDRs have helped to change the picture of molecular cloud cores from one of simple spherical blobs with thin UV-influenced external layers to one in which UV radiation affects the outer layers of dense clumps well inside the central regions of the cores.

We are grateful for the contributions of our collaborators R. Genzel, A. Harris, G. Stacey, and J. Stutzki. This work was supported in part by the National Science Foundation under grant AST 88-15801 and by NASA under grant NAG 2-419 to the University of Texas at Austin.

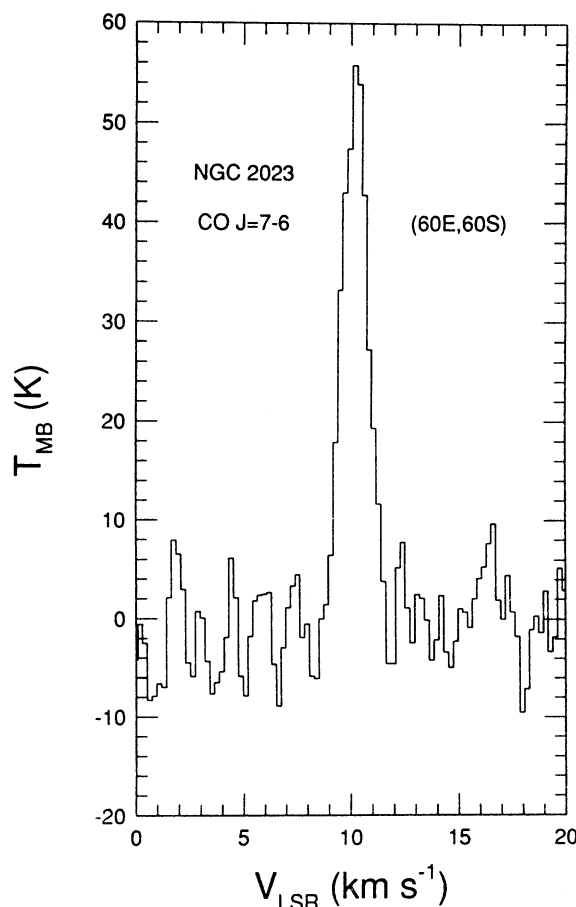


Fig. 6.: CO J = 7–6 spectrum in NGC 2023 toward a position 60 arcsec east and 60 arcsec south of HD 37903.

REFERENCES

- Black, J.H. and van Dishoeck, E.F. 1987, *Ap. J.*, **322**, 412.
 Boreiko, R.T., Betz, A.L., and Zmuidzinas, J. 1988, *Ap. J. (Letters)*, **325**, L47.
 Burton, M., Hollenbach, D., and Tielens 1988, preprint.
 Chokshi, A., Tielens, A.G.G.M., Werner, M.W., and Castelaz, M.W. 1988, *Ap. J.*, **334**, 803.
 Crawford, M.K., Genzel, R., Townes, C.H., and Watson, D.M. 1985, *Ap. J.*, **291**, 755.
 Dalgarno, J. and McCray, R. A. 1972, *Ann. Rev. Astr. and Ap.*, **10**, 375.
 Dinerstein, H.L., Lester, D.F., Carr, J.S., and Harvey, P.M. 1988, *Ap. J. (Letters)*, **327**, L27.
 Frerking, M.A., Keene, J., Blake, G.A., and Phillips, T.G. 1989, *Ap. J.*, in press.
 Gatley, I. *et al.* 1987, *Ap. J. (Letters)*, **318**, L73.
 Genzel, R., Harris, A.I., Jaffe, D.T., and Stutzki, J. 1988, *Ap. J.*, **332**, 1049.
 Genzel, R., Watson, D.M., Crawford, M.K., and Townes, C.H. 1985, *Ap. J.*, **297**, 766.
 Gerola, H., and Glassgold, A.E. 1978, *Ap. J. Suppl.*, **37**, 1.
 Graedel, T.E., Langer, W.D., and Frerking, M.A. 1982, *Ap. J. Suppl.*, **48**, 321.
 Habing, H.J. 1968, *Bull. Astr. Inst. Netherlands*, **19**, 421.
 Harris, A. I., Stutzki, J., Genzel, R., Lugten, J. B., Stacey, G. J., and Jaffe, D. T. 1987, *Ap. J. (Letters)*, **322**, 649.
 Hollenbach, D. 1988, *Astr. Lett. and Communications*, **26**, 191.
 Howe, J.E., Jaffe, D.T., Geis, N., Genzel, R., Poglitsch, A., and Stacey, G.J. 1989, *in preparation*.
 Iglesias, E. 1977, *Ap. J.*, **218**, 697.

- Jaffe, D.T., and Fazio, G.G. 1982, *Ap. J. (Letters)*, **257**, L77.
 Jaffe, D.T., Harris, A.I., Stutzki, J. and Genzel, R. 1989a, *Ap. J.*, in press.
 Jaffe, D.T., Howe, J.E., Genzel, R., Harris, A.I., Stutzki, J., and Stacey, G.J. 1989b, *in preparation*.
 Keene, J., Blake, G.A., Phillips, T.G., Huggins, P.J., and Beichman, C.A. 1985, *Ap. J.*, **299**, 967.
 Langer, W.D. 1976, *Ap. J.*, **210**, 328.
 Lugten, J.B., Watson, D.M., Crawford, M.K., and Genzel, R. 1986, *Ap. J. (Letters)*, **311**, L51.
 Makinen, P., Harvey, P.M., Wilking, B.A., and Evans, N.J. II 1985, *Ap. J.*, **299**, 341.
 Pankonin, V. and Walmsley, C.M. 1976, *Astr. and Ap.*, **48**, 341.
 Phillips, T.G. and Huggins, P.J. 1981, *Ap. J.*, **251**, 533.
 Russell, R.W., Melnick, G., Smeyers, S.D., Kurtz, N.T., Gosnell, T.R., Harwit, M., and Werner, M.W. 1981, *Ap. J. (Letters)*, **250**, L35.
 Schmid-Burgk, J. *et al.*, 1989, *Astr. and Ap.*, in press.
 Sellgren, K. 1986, *Ap. J.*, **305**, 399.
 Snell, R. L., Mundy, L. G., Goldsmith, P. F., Evans, N. J. II, and Erickson, N. R. 1984, *Ap. J.*, **276**, 625.
 Spitzer, L. 1948, *Ap. J.*, **107**, 6.
 Stacey, G.J., Smyers, S.D., Kurtz, N.T., and Harwit, M. 1983, *Ap. J. (Letters)*, **265**, L7.
 Stacey, G.J., Viscuso, P.J., Fuller, C.E., and Kurtz, N.T. 1985, *Ap. J.*, **289**, 803.
 Sternberg, A. 1986, *PhD Thesis*, Columbia University.
 Stutzki, J. and Guesten, R. 1989, *personal communication*.
 Stutzki, J., Stacey, G.J., Genzel, R., Harris, A.I., Jaffe, D.T., and Lugten, J.B. 1988, *Ap. J.*, **332**, 379.
 Tielens, A.G.G.M. and Hollenbach, D. 1985, *Ap. J.*, **291**, 722.
 van Dishoeck, E.F., and Black, J.H. 1988, *Ap. J.*, **334**, 771.
 Watson, W.D. 1972, *Ap. J.*, **176**, 103.

J.E. Howe and D.T. Jaffe: Department of Astronomy, University of Texas, 15.308 R.L. Moore Hall,
 Austin, TX 78712, USA